Calpain inhibitor and ibudilast rescue β cell functions in a cellular model of Wolfram syndrome

Lien D. Nguyen[a,b,1], Tom T. Fischer[a,c,1], Damien Abreu[d,e], Alfredo Arroyo[a], Fumihiko Urano[d,f], and Barbara E. Ehrlich[a,b,2]

[a]Department of Pharmacology, Yale University, New Haven, CT 06520; [b]Interdepartmental Neuroscience Program, Yale University, New Haven, CT 06520; [c]Institute of Pharmacology, University of Heidelberg, 69117 Heidelberg, Germany; [d]Department of Medicine, Division of Endocrinology, Metabolism, and Lipid Research, Washington University School of Medicine, St. Louis, MO 63110; [e]Medical Scientist Training Program, Washington University School of Medicine, St. Louis, MO 63110; and [f]Department of Pathology and Immunology, Washington University School of Medicine, St. Louis, MO 63110

Edited by Melanie H. Cobb, University of Texas Southwestern Medical Center, Dallas, TX, and approved June 1, 2020 (received for review April 18, 2020)

Wolfram syndrome is a rare multisystem disease characterized by childhood-onset diabetes mellitus and progressive neurodegeneration. Most cases are attributed to pathogenic variants in a single gene, Wolfram syndrome 1 (*WFS1*). There currently is no disease-modifying treatment for Wolfram syndrome, as the molecular consequences of the loss of WFS1 remain elusive. Because diabetes mellitus is the first diagnosed symptom of Wolfram syndrome, we aimed to further examine the functions of WFS1 in pancreatic β cells in the context of hyperglycemia. Knockout (KO) of WFS1 in rat insulinoma (INS1) cells impaired calcium homeostasis and protein kinase B/Akt signaling and, subsequently, decreased cell viability and glucose-stimulated insulin secretion. Targeting calcium homeostasis with reexpression of WFS1, overexpression of WFS1's interacting partner neuronal calcium sensor-1 (NCS1), or treatment with calpain inhibitor and ibudilast reversed deficits observed in WFS1-KO cells. Collectively, our findings provide insight into the disease mechanism of Wolfram syndrome and highlight new targets and drug candidates to facilitate the development of a treatment for this disorder and similar diseases.

diabetes | calcium signaling | cell viability | Akt | ibudilast

Wolfram syndrome is an orphan autosomal recessive genetic disorder that affects approximately 1 in 500,000 people worldwide and is characterized by diabetes insipidus, diabetes mellitus, optic nerve atrophy, and deafness (hence the acronym DIDMOAD) (1). Typically, a progressive childhood-onset of nonautoimmune, insulin-dependent diabetes mellitus is the first diagnosed symptom at around age 6 y (2). There is currently no disease-modifying treatment for Wolfram syndrome, and patients usually die in mid-adulthood (3). Up to 90% of cases can be attributed to pathogenic variants in the Wolfram syndrome 1 (*WFS1*) gene, which encodes for the protein wolframin (WFS1) (4). The remaining cases are due to mutations in the *CISD2* gene (a.k.a. *WFS2*) or other unknown genes (2). Heterozygous carriers of *WFS1* sequence variants compose approximately 1% of the world's population and are at enhanced risk of psychiatric disorders and hearing loss (5–7). WFS1 is a transmembrane protein and appears to localize to the endoplasmic reticulum (ER) (8). It is expressed in most tissues but at higher levels in the brain, heart, and pancreatic β cells (9). Although the endogenous functions of WFS1 remain unclear, several recent studies have suggested that WFS1 regulates ER stress (10, 11), mitochondrial health (12), and calcium homeostasis (13–15).

This study further investigates how WFS1 regulates calcium homeostasis in the context of diabetes mellitus. Calcium is a universal second messenger, and its concentration in the different cellular compartments must be tightly regulated for proper cell functions (16). In particular, intact calcium homeostasis is integral to the survival of pancreatic β cells (17, 18) and insulin secretion from these cells (19–21). In addition, dysregulation of calcium signaling has been proposed as a mechanism of many diseases, such as Alzheimer's disease (22), cancer progression (23), and diabetes mellitus (24, 25).

Here we show that KO of WFS1 in rat insulinoma (INS1) cells led to elevated resting cytosolic calcium, reduced stimulus-evoked calcium signaling, and, consequently, hypersusceptibility to hyperglycemia and decreased glucose-stimulated insulin secretion. Overexpression of WFS1 or WFS1's interacting partner neuronal calcium sensor-1 (NCS1) reversed the deficits observed in cells lacking WFS1. Moreover, calpain inhibitor XI and ibudilast rescued resting cytosolic calcium, cell viability, and insulin secretion in WFS1-KO cells. These findings further our understanding of Wolfram syndrome and other diseases caused by impaired calcium homeostasis.

Results

Loss of WFS1 Disrupts Cellular Calcium Homeostasis. Several studies have implicated a role for WFS1 in regulating calcium homeostasis, including resting cytosolic calcium (12, 14), ER calcium storage (13), and agonist-induced ER calcium release (12, 15). To study the effects of WFS1 depletion on calcium homeostasis in pancreatic β cells, we compared stable INS1 832/13 rat insulinoma cell lines with normal expression (WFS1-WT) or loss of WFS1 (WFS1-KO). Two WFS1-KO clones were created using clustered regularly interspaced short palindromic repeats (CRISPR) with a guide RNA (gRNA) targeting an early, conserved exon (*SI Appendix*, Fig. S1). All experimental results shown were obtained from WFS1-KO clone 1, and key findings were validated in WFS1-KO clone 2 (*SI Appendix*, Fig. S3). The

Significance

Wolfram syndrome is a rare multisystem disease characterized by diabetes insipidus, diabetes mellitus, optic nerve atrophy, and deafness (DIDMOAD). It is primarily caused by mutations in the Wolfram syndrome 1 gene, *WFS1*. As a monogenetic disorder, Wolfram syndrome is a model for diabetes and neurodegeneration. There is no effective treatment for this invariably fatal disease. Here we characterize WFS1 as a regulator of calcium homeostasis and subsequently target calcium signaling to reverse deficits in a cellular model of Wolfram syndrome.

Author contributions: L.D.N., T.T.F., and B.E.E. designed research; L.D.N. and T.T.F. performed research; D.A., A.A., and F.U. contributed new reagents/analytic tools; L.D.N. and T.T.F. analyzed data; and L.D.N., T.T.F., and B.E.E. wrote the paper.

Competing interest statement: B.E.E. is a cofounder of Osmol Therapeutics, a company that is targeting NCS1 for therapeutic purposes.

This article is a PNAS Direct Submission.

[1]L.D.N. and T.T.F. contributed equally to the work.

[2]To whom correspondence may be addressed. Email: barbara.ehrlich@yale.edu.

This article contains supporting information online at https://www.pnas.org/lookup/suppl/doi:10.1073/pnas.2007136117/-/DCSupplemental.

First published July 6, 2020.

WFS1-WT cell line was obtained from a clone with no CRISPR modification in the same preparation. We also generated stable WFS1-overexpressing (WFS1-OE) cells on the WFS1-KO background for validation experiments. Loss of WFS1 in WFS1-KO cells, as well as the successful reexpression of WFS1, was verified using Western blot analysis (Fig. 1*A* and *SI Appendix*, Fig. S1*E*).

To confirm a previous observation that INS1 cells with reduced WFS1 expression show higher resting cytosolic calcium levels (14), we measured resting cytosolic calcium in both cell lines using the ratiometric cytosolic calcium dye Fura-2-AM. As expected, WFS1-KO cells showed an elevated resting cytosolic calcium level at baseline compared with WFS1-WT cells, which was normalized by reexpressing WFS1 (Fig. 1*B*). Similar results were obtained using the nonratiometric cytosolic calcium dye Fluo-4-AM (*SI Appendix*, Fig. S2*A*). We also found that calpain activity was elevated in WFS1-KO cells (Fig. 1*C*), suggesting that our WFS1-KO cells recapitulate the deficits observed in an earlier WFS1-knockdown cell model (14).

WFS1-KO cells show decreased inositol 1,4,5-trisphosphate receptor-dependent ER calcium release. Because the loss of WFS1 expression has been linked to increased ER stress (10, 11) and reduced ER calcium release (12, 15), we next investigated agonist-induced calcium release from the ER in WFS1-WT and WFS1-KO cells. To measure ER calcium release via the inositol 1,4,5-trisphosphate-receptor (InsP3R), we used adenosine triphosphate (ATP) as the agonist for cells in calcium-free buffer. Measurements with Fura-2-AM dye showed reduced ATP-induced InsP3R-dependent ER calcium release into the cytosol in WFS1-KO cells (Fig. 1*D*). Compared with the WFS1-WT cells, WFS1-KO cells exhibited a significant reduction in the maximum amplitude, area under the curve, and rate of rise (Fig. 1 *E*–*G*). Similar observations were made when cells were loaded with Fluo-4-AM dye (*SI Appendix*, Fig. S2 *E*–*H*). Reintroducing WFS1 into WFS1-KO cells fully rescued the maximum amplitude and rate of rise (Fig. 1 *E*–*G*) and partially rescued the area under the curve (Fig. 1*F*). Several effects of the loss of WFS1 on ER calcium filling have been described in different cell lines (13, 15). In INS1 cells, ER calcium loading, as assessed by treatment with 1 μM thapsigargin, was not altered following the loss of WFS1 (*SI Appendix*, Fig. S2 *B*–*D*). Furthermore, the protein expressions of InsP3R1 and InsP3R3 were not different between WFS1-WT and WFS1-KO cells (*SI Appendix*, Fig. S2 *I*–*K*).

WFS1-KO cells show decreased ER-mitochondrial calcium transfer. The ER releases calcium via the InsP3R not only into the cytosol, but also into mitochondria at specialized interorganellar junctions called mitochondria-associated ER membranes (MAMs) (26). Dysregulation of MAMs has been implicated in Alzheimer's disease (27), diabetes mellitus (28, 29), and Wolfram syndrome (15). Therefore, we hypothesized that reduced cytosolic InsP3R-dependent calcium transients (Fig. 1 *D*–*G*) would be correlated with a reduction in mitochondrial calcium uptake in WFS1-KO cells. As expected, mitochondrial calcium uptake, as measured with the calcium sensor mito-gCaMP6F, was significantly lower in WFS1-KO cells after stimulation with ATP (Fig.1 *H*–*K*). Using two independent cellular fractionation protocols, we found that WFS1 was present in the crude mitochondrial fraction, which

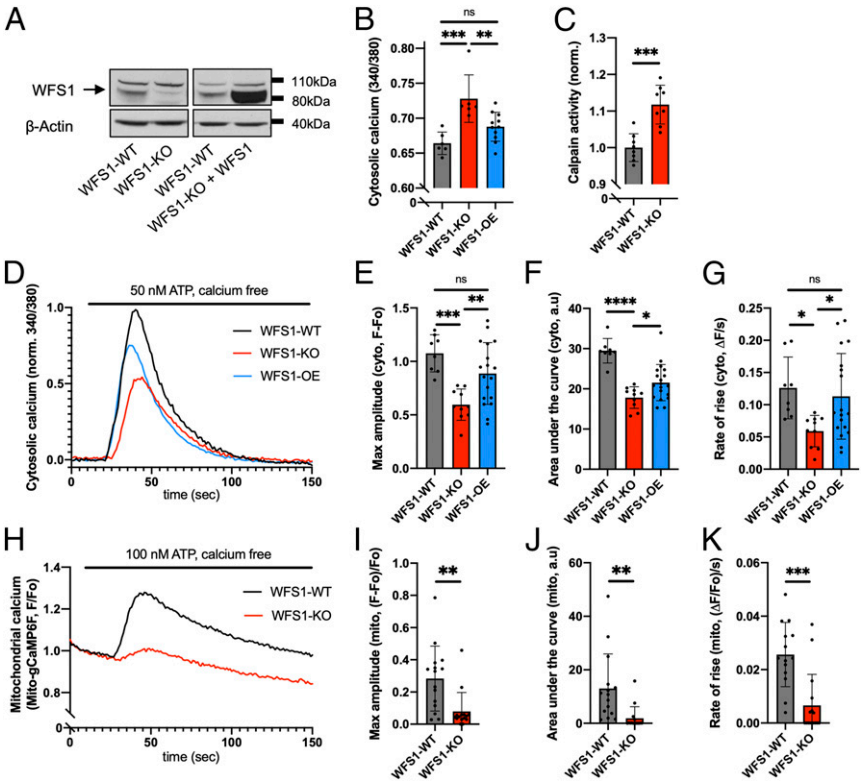

Fig. 1. WFS1 regulates intracellular calcium homeostasis in INS1 cells. (*A*) Western blot confirming the loss of WFS1 protein in WFS1-KO cells and the reexpression of WFS1 in WFS1-KO cells (WFS1-OE). (*B*) WFS1-KO cells exhibited significantly elevated resting cytosolic calcium compared with WFS1-WT cells, which could be rescued by reexpressing WFS1. (*C*) WFS1-KO cells showed significantly higher calpain activity than WFS1-WT cells. (*D*) Averaged traces of 8 to 18 coverslips for each cell type in response to 50 nM ATP. (*E*–*G*) Compared with WFS1-WT cells, WFS1-KO cells showed decreased maximum amplitude, area under the curve, and rate of rise for the cytosolic calcium traces shown in *D*. Reexpressing WFS1 fully rescued the maximum amplitude and rate of rise and partially rescued area under the curve. (*H*) Averaged traces of 15 coverslips for each cell type (both WFS1-WT and WFS1-KO cells stably expressing mito-gCaMP6F) in response to 100 nM ATP. (*I*–*K*) Compared with WFS1-WT cells, WFS1-KO cells showed decreased maximum amplitude, area under the curve, and rate of rise for the mitochondrial calcium traces shown in *H*.

contains MAM proteins (*SI Appendix*, Fig. S2 *L* and *M*). This observation is consistent with several previously published proteomic analyses of the MAM structure (30–32), supporting a role of WFS1 at the MAM.

WFS1-KO Cells Show More Severely Impaired Calcium Signaling due to Hyperglycemia. Chronic hyperglycemia, or glucose toxicity, is a hallmark of diabetes mellitus and impairs β cell physiology, particularly intracellular calcium signaling (19, 33–35). To mimic glucose toxicity in Wolfram syndrome, we treated both WFS1-WT and WFS1-KO cells with additional 30 mM glucose for 24 h before calcium imaging was performed. In the high-glucose environment, resting cytosolic calcium in WFS1-WT cells rose significantly to a level comparable to that in WFS1-KO cells at baseline (Fig. 2*A*). In contrast, resting cytosolic calcium in WFS1-KO cells treated with extra glucose remained at the same level as that in untreated WFS1-KO cells, suggesting that untreated WFS1-KO cells had already achieved a maximal resting cytosolic calcium level. In response to increasing glucose concentrations (+0, 15, or 30 mM glucose for 24 h), both WFS1-WT and WFS1-KO cells showed a concentration-dependent reduction in ATP-evoked ER calcium release into the cytosol (Fig. 2*B*). Nevertheless, WFS1-KO cells showed a lower calcium response at 0 mM and 15 mM additional glucose compared with WFS1-WT cells at the same concentrations. The response for both cell lines converged to a minimal level at the highest glucose concentration tested (+30 mM).

Further analyses of maximum amplitude, area under the curve, and rate of rise suggest that WFS1-KO cells at baseline showed an ATP response similar to that in WFS1-WT cells treated with 15 mM glucose, and that WFS1-KO cells treated with 15 mM showed a similar response as WFS1-WT cells treated with 30 mM glucose (Fig. 2 *C*–*E*). These observations indicate that at baseline, WFS1-KO cells already show defects in calcium signaling comparable to those in WFS1-WT cells under diabetic hyperglycemia, which may result in an acceleration of functional impairments following hyperglycemia in WFS1-KO cells.

Overexpression of WFS1's Interacting Partner NCS1 Rescues Calcium Homeostasis in WFS1-KO Cells. Neuronal calcium sensor-1 (NCS1) is a regulator of calcium-dependent signaling pathways (36), such as survival (37) and insulin secretion (38), and was recently implicated in the disease mechanism of Wolfram syndrome in fibroblasts (15). WFS1 and NCS1 interaction has been reported previously, which we corroborated with coimmunoprecipitation experiments (Fig. 3*A*). Unlike what was previously observed in fibroblasts, we saw no difference in NCS1 protein expression between INS1 WFS1-WT and WFS1-KO cells, suggesting tissue-specific regulation (*SI Appendix*, Fig. S4 *A* and *B*). Given reports indicating that NCS1 protein expression is increased in response to cell stress (37, 39), we assessed NCS1 protein expression following hyperglycemia. We found that glucose toxicity led to an approximate 1.5-fold increase in NCS1 protein expression in WFS1-WT cells after 48 h (Fig. 3 *B* and *C*). In contrast, in WFS1-KO

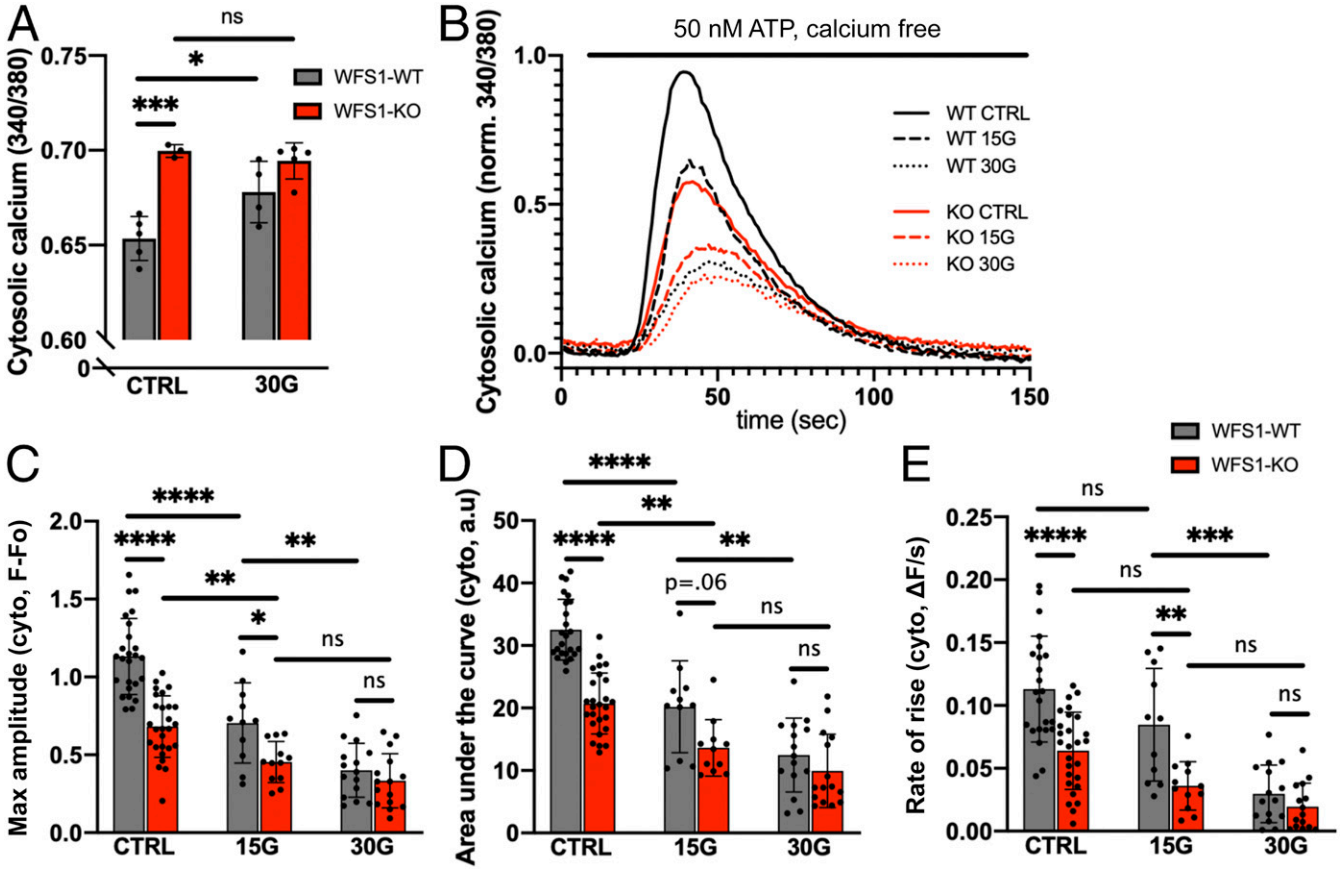

Fig. 2. WFS1-KO cells show more severely impaired calcium signaling due to hyperglycemia. Cells were incubated for 24 h with normal medium (CTRL) or medium with 15 mM or 30 mM additional glucose (15G and 30G, respectively) before imaging. (*A*) WFS1-WT cells showed elevated resting cytosolic calcium after incubation with 30G, whereas WFS1-KO cells showed no change. (*B*) Averaged traces of 12 to 25 coverslips for each condition in response to 50 nM ATP. (*C*–*E*) Quantification of maximum amplitude, area under the curve, and rate of rise for the cytosolic calcium traces shown in *B*. Glucose toxicity caused impairment of ATP-evoked calcium transients in a concentration-dependent manner. However, WFS1-KO cells showed a more impaired response at CTRL and 15G. At 30G, WFS1-WT and WFS1-KO cells were equally impaired.

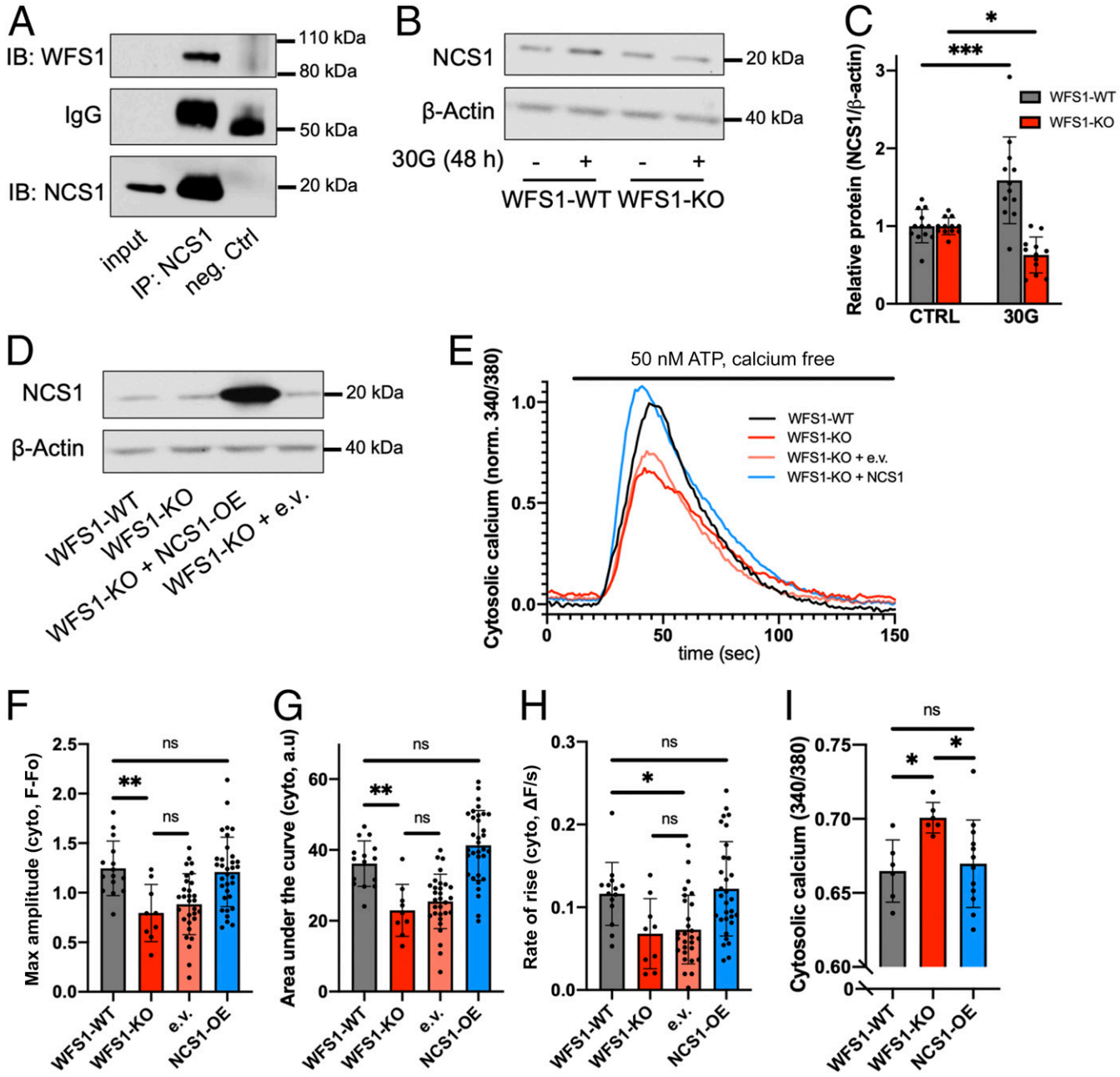

Fig. 3. Overexpression of WFS1's interacting partner NCS1 rescues calcium homeostasis in WFS1-KO cells. (*A*) For coimmunoprecipitation, mouse brain lysate was incubated with NCS1 antibody or rabbit IgG as control. Immunoblots were incubated with antibodies as indicated. (*B*) Representative blot showing protein abundance of NCS1 in WFS1-WT and WFS1-KO cells treated for 48 h with an additional 30 mM glucose (30G). (*C*) Quantification of *B* (10 to 12 independent preparations for each condition), with values normalized to CTRL. Whereas WFS1-WT cells showed an increase in NCS1 level, WFS1-KO cells showed a decrease. (*D*) Western blot confirming the overexpression of NCS1 in WFS1-KO cells. (*E*) Averaged traces of 9 to 32 coverslips for each cell type in response to 50 nM ATP. Overexpression of NCS1 rescued ATP-evoked cytosolic calcium response in WFS1-KO cells. (*F–H*) Quantification of maximum amplitude, area under the curve, and rate of rise for the cytosolic calcium traces shown in *E*. (*I*) Overexpression of NCS1 rescued elevated resting cytosolic calcium in WFS1-KO cells.

cells, a significant decrease in NCS1 protein expression was observed (Fig. 3 *B* and *C*). NCS1 mRNA level was not changed between the different conditions (*SI Appendix*, Fig. S4*C*), indicating that WFS1 likely regulates NCS1 protein levels posttranscriptionally.

Next, we overexpressed NCS1 in WFS1-KO cells and found that NCS1 overexpression fully rescued both the ATP-evoked ER calcium release (Fig. 3 *E–H*) and the resting cytosolic calcium (Fig. 3*I*). Overexpressing the empty vector with a green fluorescence protein (GFP) marker alone did not affect calcium response in WFS1-KO cells, suggesting that neither the transfection process nor the GFP signal interfered with our measurement. Consistent with a previous study (15), these results indicate that NCS1 plays a role in the disease mechanism of Wolfram syndrome and is a potential target for treatment, as has been reported for other conditions (40, 41).

Calpain Inhibitor XI and Ibudilast Rescue Cell Viability and Resting Cytosolic Calcium in WFS1-KO Cells. Because intracellular calcium is an important determinant of cell viability, we measured cell viability in WFS1-WT and WFS1-KO cells using a luminescent

ATP-based assay. First, we established that knocking out WFS1 in INS1 cells did not reduce cell viability at baseline (Fig. 4*A*) or proliferation over 1 wk (Fig. 4*B*). Following hyperglycemia (additional 30 mM glucose for 48 h), we observed an ∼40% reduction in cell viability in WFS1-KO cells, compared with only a 15% reduction in WFS1-WT cells (Fig. 4*C*). The reduction in viability in WFS1-KO cells could be rescued by WFS1 reexpression (*SI Appendix*, Fig. S5*A*). These findings are supported by previous reports showing that WFS1 deficiency causes progressive loss of pancreatic β cells (42, 43).

Calpain inhibitor and ibudilast rescue cell viability in WFS1-KO cells. To reverse the hyperglycemia-induced loss of cell viability pharmacologically, six different compounds previously shown to affect calcium homeostasis and WFS1- or NCS1-dependent processes were tested in WFS1-WT, WFS1-KO, and WFS1-OE cells (*SI Appendix*, Fig. S5*A*). Two of these compounds, calpain inhibitor XI (also known as AK295 or CX295) and ibudilast (also known as AV-411 or MN-166), fully rescued cell viability back to baseline in all three cell lines. Subsequently, we found that calpain inhibitor XI and ibudilast did not significantly affect cell viability at baseline (Fig. 4*C*) and reversed the glucose toxicity-induced loss of cell viability in a dose-dependent manner in WFS1-KO cells (*SI Appendix*, Fig. S5 *B*–*E*). Calpain inhibitor XI is a reversible inhibitor of calpain 1 and 2 (44) and shows antiapoptotic/prosurvival properties in models of several diseases in vitro and in vivo (45–50). Ibudilast was developed as a phosphodiesterase 4 (PDE4) inhibitor and is approved in Japan for the treatment of patients with asthma and poststroke dizziness (51).

Calpain inhibitor and ibudilast rescue resting cytosolic calcium in WFS1-KO cells. To investigate a possible mechanism of drug action, we tested whether calpain inhibitor XI and ibudilast could rescue resting cytosolic calcium following the loss of WFS1. A sustained elevation in resting cytosolic calcium level can lead to harmful cellular processes resulting in cell death (16) and impaired insulin secretion (19). Both calpain inhibitor XI and ibudilast lowered the resting cytosolic calcium level in WFS1-KO cells to that in WFS1-WT cells (Fig. 4 *D* and *E*), underscoring that disrupted calcium signaling is an important contributor to Wolfram syndrome pathology and can be targeted with calpain inhibitor XI and ibudilast.

WFS1-KO Cells Show Decreased Insulin Secretion, Which Can Be Reversed by Calpain Inhibitor XI and Ibudilast. In addition to reduced β cell mass (Fig. 4), decreased glucose-stimulated insulin secretion has been observed in studies investigating animal models with WFS1 deficiency and corresponding pancreatic islets (43, 52, 53). Measurement of glucose-stimulated insulin secretion showed that stimulation with 9 mM glucose significantly increased insulin secretion in WFS1-WT cells but not in WFS1-KO cells (Fig. 5*A*). This

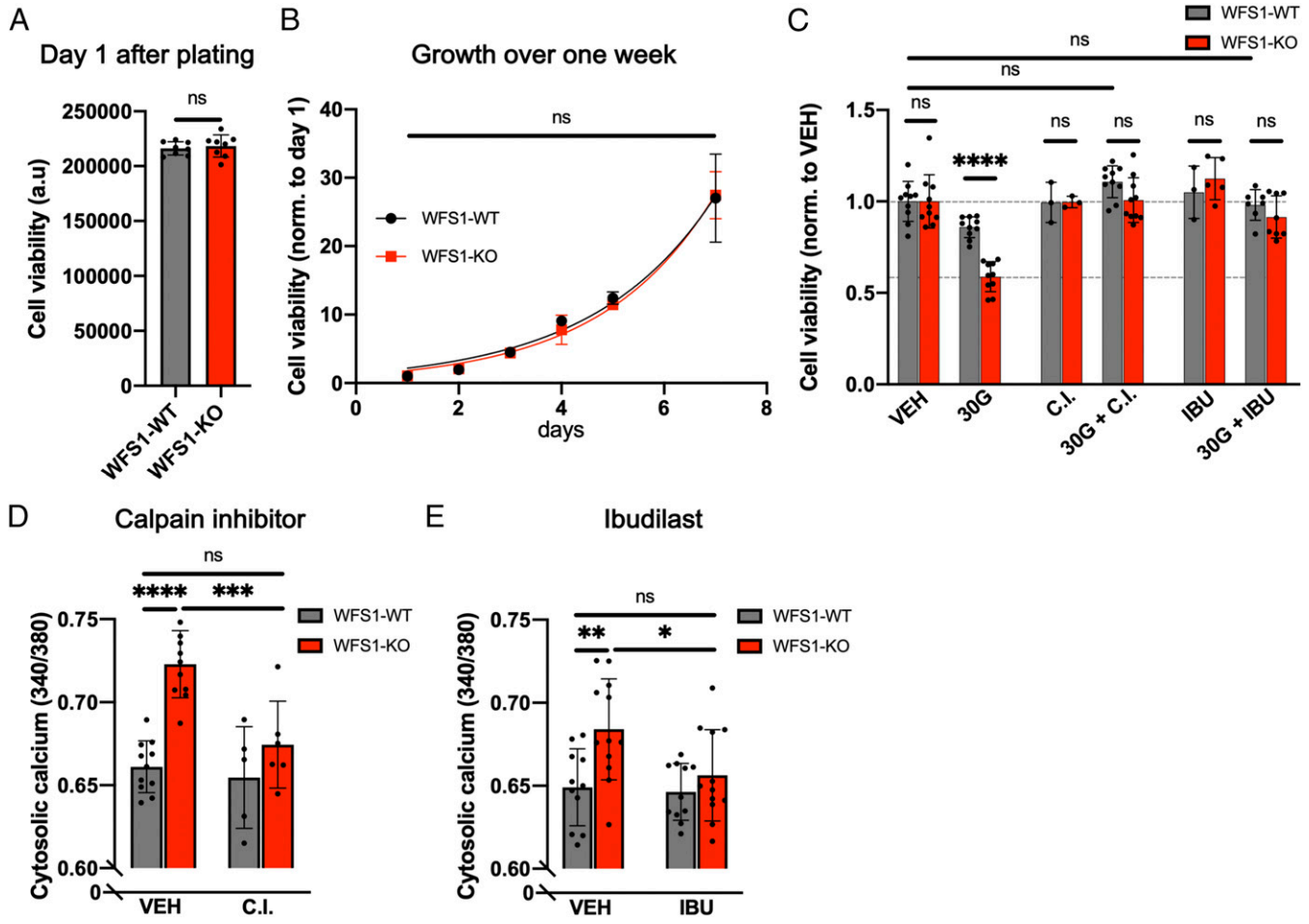

Fig. 4. Calpain inhibitor XI and ibudilast rescue cell viability and resting cytosolic calcium in WFS1-KO cells. (*A*) Measurement of cell viability of WFS1-WT and WFS1-KO cells showed no difference under control conditions on day 1. (*B*) Measurement of growth over 7 d showed no difference between WFS1-WT and WFS1-KO cells. (*C*) Measurement of cell viability normalized to CTRL conditions. WFS1-KO cells showed a significantly larger reduction in cell viability compared with WFS1-WT cells. Cell viability in both cell lines was rescued by 10 μM calpain inhibitor XI (CI) and 10 μM ibudilast (IBU). Treatment combinations were as indicated for 48 h. (*D* and *E*) A 24-h treatment with 10 μM CI or IBU reversed elevated cytosolic calcium levels in WFS1-KO cells without affecting WFS1-WT cells.

resulted in a significantly lower insulin secretion rate in WFS1-KO cells compared with WFS1-WT cells at 9 mM glucose. Adding either calpain inhibitor XI or ibudilast reversed the impairment of glucose-stimulated insulin secretion in WFS1-KO cells. Treatment with calpain inhibitor XI did not affect insulin secretion in WFS1-WT cells and rescued secretion in WFS1-KO cells. Similar to another PDE4 inhibitor, roflumilast (54), ibudilast enhanced insulin secretion at baseline in both cell lines. Following glucose stimulation, ibudilast ameliorated the difference between WFS1-WT and WFS1-KO cells.

WFS1-KO cells show decreased insulin receptor and protein kinase B/Akt signaling. Studies performed in animal models lacking the insulin receptor (IR) and insulin-like growth factor I (IGF1) receptor indicate that insulin also exerts an important effect on β cells, and that IR signaling regulates survival and insulin secretion in β cells (55–57). Therefore, we examined the expression levels of proteins involved in the insulin signaling network. Total IR and protein kinase B (Akt) were similar among the WFS1-WT, WFS1-KO, and WFS1-OE cells (Fig. 5*B* and *SI Appendix*, Fig. S6 *A* and *B*). Phosphorylation of the insulin receptor (pIRβ-Y1150/1151) and Akt (pS473 and pT308) was significantly reduced in WFS1-KO cells (Fig. 5 *B–F*). Reintroducing WFS1 in WFS1-KO cells significantly increased pIRβ-Y1150/1151 and rescued pAkt-S473. These data suggest that disruption of IR and Akt signaling plays a role in Wolfram syndrome pathology.

Discussion

WFS1 Regulates Intracellular Calcium Homeostasis. Here we describe how intracellular calcium is globally dysregulated in WFS1-KO β cells. Consistent with previous studies in the field (12, 14, 15, 25), WFS1-KO cells showed elevated resting cytosolic calcium and reduced ATP-evoked calcium transients from the ER to both the cytosol and mitochondria. The exact mechanism of WFS1-dependent InsP3R dysfunction is unclear; however, we were able to rule out reduced expression of InsP3Rs or decreased ER-calcium loading as causes. There remain several possible and not mutually exclusive explanations. First, WFS1 may interact directly with the InsP3R (15) and positively regulate InsP3R function similar to NCS1 (58, 59). Second, WFS1 may function as a calcium-permeable ion channel (60). Taken together, our data on calcium signaling in a cellular disease model of Wolfram syndrome emphasize that WFS1 is a versatile regulator of calcium homeostasis.

WFS1-KO cells are predisposed to hyperglycemia-induced impairments. When cells were challenged with glucose toxicity, WFS1-KO cells showed more severely impaired calcium signaling compared with WFS1-WT cells. Similar to wild-type rat islet cells that had been cultured in high glucose over 1 wk (33), WFS1-KO cells showed no further increase in resting cytosolic calcium level. Therefore, we propose that at baseline, WFS1-KO cells already

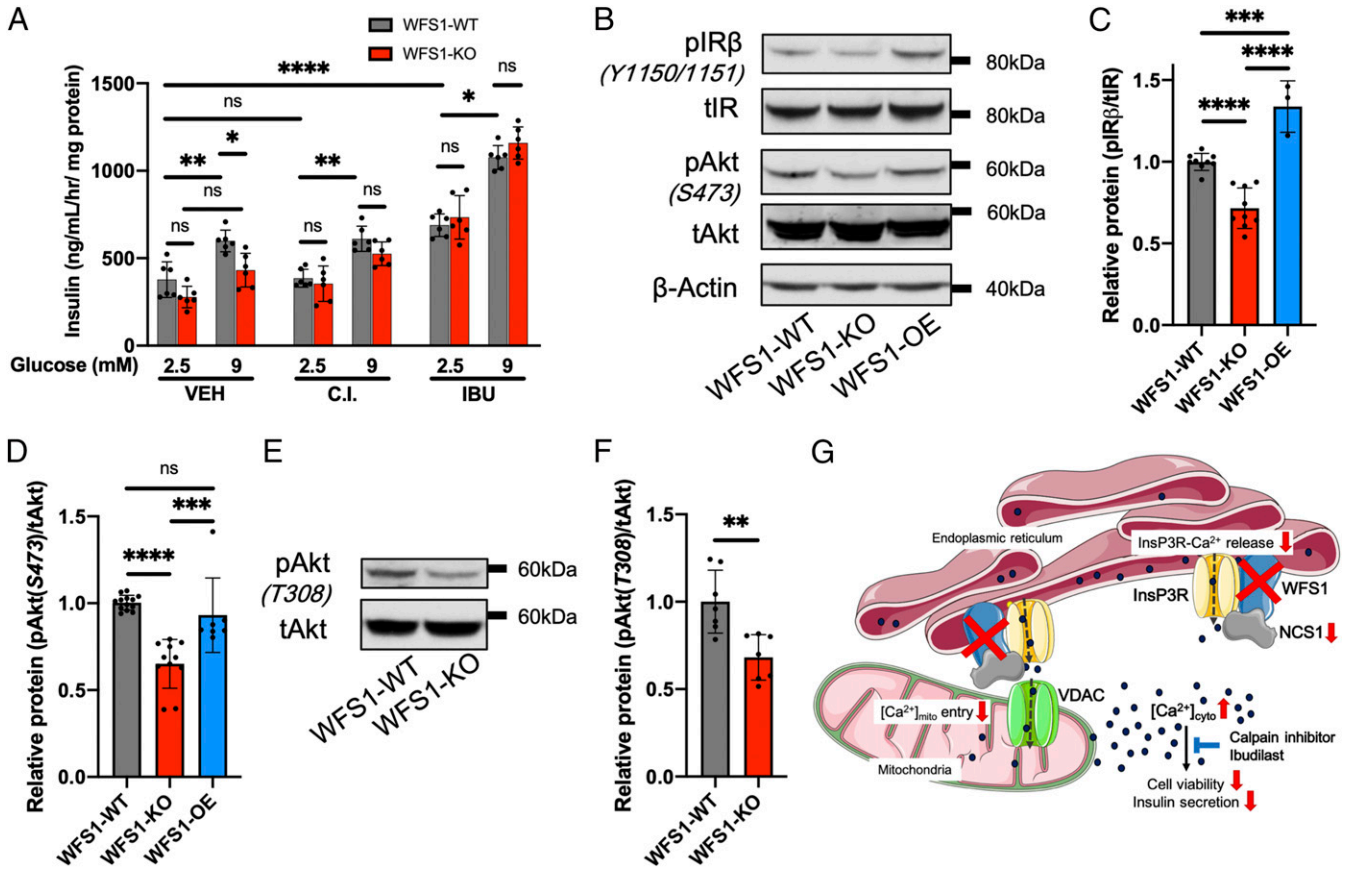

Fig. 5. WFS1-KO cells show decreased insulin secretion, which can be reversed by calpain inhibitor XI and ibudilast. (*A*) Measurement of glucose-stimulated insulin secretion at baseline (2.5 mM glucose) and after stimulation (9 mM glucose) using insulin ELISA. WFS1-WT cells showed significantly higher insulin secretion than WFS1-KO cells under control conditions. Treatment with 10 μM calpain inhibitor XI or 10 μM ibudilast ameliorated the difference between WFS1-WT and WFS1-KO cells. (*B*) Representative blot showing protein abundance of the insulin signaling pathway. (*C* and *D*) Quantification of A (3 to 10 independent preparations). Compared with WFS1-WT cells, WFS1-KO showed significant reductions in pIRβ (Y1150/1151) and pAKT (S473). Reexpression of WFS1 in WFS1-KO cells increased pIRβ and pAKT expression levels to at least those in WFS1-WT cells. (*E*) Representative blot showing protein abundance of pAKT (T308). (*F*) Quantification of D (seven independent preparations). pAKT (T308) was significantly down-regulated in WFS1-KO cells. (*G*) Proposed model. Loss of WFS1 results in global calcium dysregulation, which impairs cell viability and insulin secretion. Calpain inhibitor XI and ibudilast can restore proper β cell function, suggesting them as drug candidates for the treatment of Wolfram syndrome and similar diseases.

show signaling impairments like "diabetic" cells. Such impairments predispose them to more severe hyperglycemia-induced defects, as supported by the lower cell viability seen in WFS1-KO cells following hyperglycemia. This may explain why patients with Wolfram syndrome develop more degenerative symptoms progressively with age.

WFS1-KO cells show impaired IR and Akt signaling. Decreased IR and Akt signaling, likely linked through defects in PI3K and mTORC2 signaling (61), may contribute to the impaired insulin secretion (62) and cell viability (63, 64) of WFS1-KO cells. Reduced protein kinase B/Akt signaling may be due to elevated cytosolic calcium level (65, 66). In addition, protein phosphatase 2A (PP2A) also reduces the phosphorylation of IR, Akt, and other insulin-signaling molecules and is known to be hyperactivated in diabetic states (67). Although we saw no changes in the protein expression of the catalytic subunit of PP2A (PP2Ac; *SI Appendix*, Fig. S6 *C* and *D*), PP2A activity is regulated by multiple factors, including calcium (68) and posttranslational modifications (67). Alternatively, the reduced insulin secretion in WFS1-KO cells may down-regulate the insulin signaling pathway. Akt signaling could be a new drug target for Wolfram syndrome, as has been previously investigated in other conditions, including obesity and type 2 diabetes mellitus (69).

Restoring Calcium Homeostasis in WFS1-KO Cells.

NCS1. We found that overexpressing NCS1 is a promising strategy to restore calcium homeostasis in INS1 cells. NCS1 may normalize calcium dysregulation through its enhancing effect on InsP3R activity (58, 59) and its function as a calcium sensor (36). Moreover, a recent study found that NCS1 was mislocalized in adipocytes of a high-fat diet mouse model (70). Therefore, we speculate that localization or functions of NCS1 are similarly altered in "diabetic" WFS1-KO cells.

Calpain inhibitor XI and ibudilast. Pharmacologic interventions with calpain inhibitor XI and ibudilast rescued resting cytosolic calcium as well as cell viability and glucose-stimulated insulin secretion of WFS1-KO cells. The specific mechanism of action for both drugs in Wolfram syndrome has yet to be determined, but we provide evidence that they act through normalizing calcium homeostasis. Calpains, which are calcium-dependent cysteine proteases, are typically regulated by changes in cytosolic calcium (71). Calpain inhibitor XI reversibly inhibits the activity of calpain-1, calpain-2, and, with a lower potency, another cysteine protease, cathepsin B (K_i = 140 nM, 41 nM, and 6.9 μM, respectively) (72). These K_i values were measured with purified enzymes. In our experiments, μM concentrations of calpain inhibitor XI were required for functional effects in intact INS1 cells, which is consistent with previous cell-based studies (45–48). Whereas a potential off-target effect on cathepsin B cannot be excluded, inhibition of calpains and cathepsin B may work synergistically as a calpain-cathepsin axis has been proposed (73). The calpain pathway should be further investigated in β cells in the context of hyperglycemia, because calpain hyperactivity has been observed in diabetic cardiomyocytes (74), and overexpression of calpastatin, the endogenous inhibitor of calpain, protects mice against diabetes (75). Our observation that calpain inhibitor XI normalized resting cytosolic calcium in WFS1-KO cells suggests feedback signaling between calcium-activated cysteine proteases and cytosolic calcium.

We hypothesize that ibudilast normalizes calcium through its interaction with NCS1 (40). Furthermore, the effect of ibudilast on PDE4—and hence cAMP levels—in WFS1-WT and WFS1-KO cells merits investigation, because cAMP interacts with calcium signaling pathways and is similarly implicated in cell viability and insulin secretion of β cells (76–78). Ibudilast has already been approved for use in humans (51) and appears to be a safe candidate for treating Wolfram syndrome. In addition to restoring β cell function, ibudilast may also reduce the neurodegenerative symptoms of Wolfram syndrome, as it is known to reduce neurotoxic symptoms (79–81) and is currently in clinical trials for multiple sclerosis (82) and amyotrophic lateral sclerosis (83).

Proposed Model and Future Directions. Dysregulation in calcium signaling has been implicated in the pathogenesis of diabetes mellitus (25, 84) and neurodegeneration (85, 86), the two hallmarks of Wolfram syndrome. Here we propose a disease model for Wolfram syndrome in which global dysregulation of intracellular calcium homeostasis disrupts associated pathways, including calpain, NCS1, and Akt, and leads to reduced cell viability and insulin secretion (Fig. 5*G*). Calpain inhibitor XI and ibudilast reversed deficits caused by the loss of WFS1, making them promising drug candidates for the treatment of Wolfram syndrome. This effect should be recapitulated in cell lines expressing WFS1-variants as seen in patients, and then further tested in an animal model of Wolfram syndrome (52, 53).

To advance our understanding of the disease mechanism of Wolfram syndrome, the link between disrupted calcium and the IR/Akt pathway should be further investigated. Importantly, the IR signaling network is increasingly recognized as an essential and druggable pathway both in β cells and the brain (87). Because Wolfram syndrome has been proposed as a model system for diabetes mellitus and neurodegenerative diseases (2), we expect that the findings presented in this paper will be relevant to many fields of research.

Materials and Methods

Reagents. All chemicals used were obtained from Sigma-Aldrich unless stated otherwise. Calpain inhibitor XI was purchased from Calbiochem; ibudilast, from Cayman Chemical Company; and ATP, from AmericanBio. Stock concentrations of drugs were prepared in 100% DMSO (AmericanBio), aliquoted, and stored at −20 °C. For treatment, stock concentrations were diluted in cell medium, and DMSO concentration was kept at <0.1% in all experiments.

Generation of Stable Cell Lines and Cell Culturing. The WFS1-KO INS1 832/13 lines were generated by the Genome Engineering and iPSC Center (GEiC) at the Washington University in St. Louis (*SI Appendix*, Fig. S1). gRNAs were designed using CRISPOR (crispor.tefor.net) to target an early exon common to all transcription isoforms, cloned under a U6 promoter, and validated for cleavage activity in rat C6 cells by cotransfecting with a plasmid expressing Cas9 under the CMV promoter (CMV-Cas9-NLS-HA). The most active gRNA (5′-*gctgctggagaatgtcgggcagg*) construct was then cotransfected with the Cas9 plasmid into INS1 cells using the nucleofection method in solution P3 and the program DS-150, following the manufacturer's (Lonza) instructions.

The transfected pool was genotyped to confirm the presence of editing at the target site before single cells were sorted into 96-well plates. Clones grown from the sorted plates were genotyped at the target site to identify those carrying out-of-frame indels in all alleles (deep sequencing analysis, primers: F: 5′-*aatacggcatagagcccatgatt*, R: 5′-*tggtctagcttgtgaagtagctg*). Then positive clones were expanded. Genotype was confirmed when cells were transferred from a six-well plate to a T75 flask. An additional frozen vial of cells was then thawed and tested to confirm good survival, and the culture was tested for mycoplasma contamination before delivery.

WFS1-OE cells were generated by transfecting WFS1-KO clone 1 cells with a pcDNA3.1 plasmid carrying the full-length WFS1 sequence (Addgene; 13011) using Lipofectamine 2000 (Thermo Fisher Scientific), followed by 4 wk of antibiotic selection with 2 mg/mL G418 (AmericanBio). WFS1-WT and WFS1-KO cells stably expressing mito-gCaMP6F (a gift from D. Stefani, University of Padua) were generated by transfection with mito-gCaMP6F using Lipofectamine 2000. GFP-positive cells were subsequently collected by fluorescence-activated cell sorting (FACS). NCS1-OE and empty vector control cells were generated by transfecting WFS1-KO clone 1 cells with a pIRES2-EGFP plasmid (a gift from E. Gracheva, Yale University) with or without the full-length NCS1 sequence using Lipofectamine 2000, then collected using FACS. All INS1 cell lines were maintained at 37 °C and 5% CO_2 in RPMI 1640 supplemented with 10% FBS, 1% Hepes, 1% sodium pyruvate, 50 μM β-mercaptoethanol, and 1% penicillin/streptomycin (Gibco). The cell medium for WFS1-OE, mito-gCaMP6F, NCS1-OE, and the empty vector control was also supplemented with 1 mg/mL G418 for maintenance.

Calcium Imaging. Here 2×10^5 cells were plated on each coverslip at 48 h before imaging in INS1 medium without G418. Hepes-buffered saline (140 mM NaCl, 1.13 mM $MgCl_2$, 4.7 mM KCl, 2 mM $CaCl_2$, 10 mM D-glucose, and 10 mM Hepes, adjusted to pH 7.4 with NaOH) was used to prepare calcium dye solution and during imaging. In calcium-free Hepes buffer, $CaCl_2$ was replaced with $MgCl_2$, and 0.1 mM EGTA was added to chelate calcium. Fura-2-AM dye powder (Thermo Fisher Scientific) was dissolved to 4 μM in calcium-containing Hepes buffer supplemented with 0.03% pluronic acid (Thermo Fisher Scientific). On the day of imaging, each coverslip was incubated in dye solution for 45 min in the dark at room temperature. Each coverslip was then washed three times in Hepes-buffered saline solution before the start of calcium imaging.

Calcium measurements were performed with a Hamamatsu Orca R2 camera attached to a Zeiss microscope with a Sutter Lambda DG4 for excitation ratio imaging. Cells were imaged using sequential excitation at 340/380 nm (Fura-2-AM). Images were acquired with an emission bandwidth of 501 to 550 nm every second. The raw 340-nm and 380-nm signals for each cell were subtracted by the corresponding background signal before a 340/380 ratio was calculated. Maximum amplitude and area under the curve were calculated using GraphPad Prism 8. The rate of rise was quantified as the gradient between 25% and 75% maximum amplitude. All experiments were conducted at room temperature. For calcium imaging at varying glucose concentrations, glucose concentration was maintained throughout the dye and imaging solutions.

For mitochondrial calcium imaging, cells stably expressing mito-gCaMP6F were prepared on coverslips as described above. Then 48 h later, the cells were imaged using sequential excitation at 488 nm, and images were acquired with an emission bandwidth of 501 to 555 nm. The experiment was carried out and analyzed similarly to the cytosolic calcium recordings, except that after background subtraction, data were normalized to the first 10 s (baseline recording). All figures depicting calcium imaging traces show the average of 8 to 24 coverslips, each with 40 to 70 cells, from at least three independent recordings.

Western Blot Analysis. Cultured cells were lysed in mammalian protein extraction reagent (MPER; Thermo Fisher Scientific). Mouse brains were lysed in radioimmunoprecipitation assay (RIPA) buffer (Santa Cruz Biotechnology). Both MPER and RIPA were supplemented with Halt protease and phosphatase inhibitor mixture (Thermo Fisher Scientific). After spinning down at 13,000 rpm for 20 min at 4 °C to clear cell lysate, the protein concentration was measured with a bicinchoninic acid assay (Thermo Fisher Scientific). Equal amounts of protein were loaded, and electrophoresis was performed in NuPAGE 4 to 12% gradient bis-Tris polyacrylamide protein gels (Thermo Fisher Scientific). Proteins were transferred to a PVDF membrane and blocked with 5% milk in PBS (AmericanBio) with 0.1% Tween-20 for 1 h. Membranes were then incubated overnight with primary antibodies (*SI Appendix*, Table S1) at 4 °C. Blots were washed and incubated with secondary antibody for 2 h at room temperature. After washing, the secondary antibody was visualized using Pierce ECL chemiluminescence reagents (Thermo Fisher Scientific) or a LI-COR Odyssey imaging system.

Coimmunoprecipitation. Here 500 μL of 1 μg/μL mouse brain lysate (in RIPA with protease and phosphatase inhibitor) was incubated with 10 μL of NCS1 antibody (FL190; Santa Cruz Biotechnology) or 10 μL of rabbit IgG overnight at 4 °C, followed by incubation with 30 μL of Pierce protein A/G magnetic beads (Thermo Fisher Scientific) for 2 h at 4 °C. Incubated beads were washed three times with cold PBS (AmericanBio) and then eluted by boiling with 20 μL of loading buffer. The eluted fractions were then analyzed via Western blot analysis.

Cell Viability Assay. A CellTiter-Glo (CTG) assay (Promega) was used to quantify ATP-dependent bioluminescence as an indicator of cell viability. To assess cell viability, INS1 cells were plated in white 96-well plates (Thermo Fisher Scientific; 07-200-628) at a density of 2×10^3 cells per well and treated the next day with high glucose and/or the indicated drugs for 48 h before imaging. On completion of treatment, 100 μL of CTG solution was added to each well, and 20 min later, a reading was performed using a Tecan Infinite M1000 Pro microplate reader with 5 s orbital shaking (3 mm, 216 rpm), followed by imaging in luminescence mode with a 500-ms integration time.

Calpain Activity Assay. The Calpain-Glo protease assay (Promega) was used to quantify calpain activity. Here 1×10^6 cells per well were plated on a 12-well plate and then lysed in CytoBuster (Novagen) 24 h later. Protein concentration was quantified using a BCA assay. The calpain assay was carried out on a white 96-well plate in a 100-μL reaction setup. In each well, 25 μg of protein was diluted in 50 μL of CytoBuster. Here 50 μL of pure CytoBuster served as a negative control, and 50 μL of CytoBuster with 2 mM $CaCl_2$ and 1 μL of pure calpain-2 served as a positive control. Finally, 50 μL of Calpain-Glo solution was added to each well and 30 min later, activity was measured using a Tecan Infinite M1000 Pro microplate reader with the same setting as described for the CTG assay.

Insulin Secretion Assay. For glucose-stimulated insulin secretion studies, INS1 cells were plated on six-well plates at a density of 6×10^5 cells per well. After 24 h, cells were incubated with drugs for another 24 h. At 48 h after plating, insulin ELISAs were performed following a previously published protocol (88). In detail, preincubation of cells in a Dulbecco's Modified Eagle's Medium (DMEM) base (Sigma-Aldrich) supplemented with 2.5 mM glucose for 1.5 h was followed by a 45-min incubation in a DMEM base with either 2.5 mM glucose for basal secretion or 9 mM glucose for stimulated secretion, as indicated. Then 200 μL of supernatant was collected for analysis of insulin concentration using the Rat High Range ELISA Kit (80-INSRTH-E01; ALPCO). Cells were washed with ice-cold PBS and lysed in 1 mL of 0.1% Triton X-100. Insulin levels were normalized to total protein as measured with the Micro BCA Protein Assay Kit (Thermo Fisher Scientific; 23235).

Data Analysis. Data management and calculations were performed using GraphPad Prism 8. Comparisons between two groups were done using the unpaired two-tailed Student *t* test. For comparison of more than two groups, one-way analysis of variance (ANOVA), followed by Tukey's post hoc test, was performed. A P value < 0.05 was considered statistically significant, and the following notations are used in all figures: $*P < 0.05$, $**P < 0.01$, $***P < 0.001$, and $****P < 0.0001$. All error bars shown represent SD. Detailed results of statistical analyses are provided in *SI Appendix*, Table S2.

Data Availability. All data needed to evaluate the conclusions in the paper are provided in main text or *SI Appendix*. All laboratory protocols are described and cited in *Materials and Methods*. Further information, as well as a list of reagents, is available on request from the corresponding author.

ACKNOWLEDGMENTS. We thank Edward Kaftan, Eiman Ibrahim, Allison Brill, Jae-Sung Yi, and Marc Freichel for helpful discussions and Xiaoyong Yang and Hannah Hausschild for comments on the manuscript. We also thank the Genome Engineering and iPSC Center (GEiC) at Washington University in St. Louis for their cell line engineering services that produced the INS1 WFS1-WT and WFS1-KO cells used in this study, and the Yale Islet, Oxygen Consumption, Mass Isotopomer Flux Core (IOMIC) for their assistance with insulin secretion measurements. This work was supported by NIH Grants P01 DK057751 (to B.E.E.); DK112921, DK020579, and TR002065 (to F.U.); and F30 DK111070 (to D.A.). T.T.F. was supported by a scholarship from the German Academic Scholarship Foundation.

1. T. G. Barrett, S. E. Bundey, Wolfram (DIDMOAD) syndrome. *J. Med. Genet.* **34**, 838–841 (1997).
2. L. Rigoli, P. Bramanti, C. Di Bella, F. De Luca, Genetic and clinical aspects of Wolfram syndrome 1, a severe neurodegenerative disease. *Pediatr. Res.* **83**, 921–929 (2018).
3. F. Urano, Wolfram syndrome: Diagnosis, management, and treatment. *Curr. Diab. Rep.* **16**, 6 (2016).
4. F. Khanim, J. Kirk, F. Latif, T. G. Barrett, WFS1/wolframin mutations, Wolfram syndrome, and associated diseases. *Hum. Mutat.* **17**, 357–367 (2001).
5. K. Inoue, J. R. Lupski, Genetics and genomics of behavioral and psychiatric disorders. *Curr. Opin. Genet. Dev.* **13**, 303–309 (2003).
6. R. G. Swift, M. H. Polymeropoulos, R. Torres, M. Swift, Predisposition of Wolfram syndrome heterozygotes to psychiatric illness. *Mol. Psychiatry* **3**, 86–91 (1998).
7. M. Swift, R. G. Swift, Psychiatric disorders and mutations at the Wolfram syndrome locus. *Biol. Psychiatry* **47**, 787–793 (2000).
8. K. Takeda *et al.*, WFS1 (Wolfram syndrome 1) gene product: Predominant subcellular localization to endoplasmic reticulum in cultured cells and neuronal expression in rat brain. *Hum. Mol. Genet.* **10**, 477–484 (2001).
9. S. Hofmann, C. Philbrook, K. D. Gerbitz, M. F. Bauer, Wolfram syndrome: Structural and functional analyses of mutant and wild-type wolframin, the WFS1 gene product. *Hum. Mol. Genet.* **12**, 2003–2012 (2003).
10. S. G. Fonseca *et al.*, WFS1 is a novel component of the unfolded protein response and maintains homeostasis of the endoplasmic reticulum in pancreatic beta-cells. *J. Biol. Chem.* **280**, 39609–39615 (2005).
11. S. G. Fonseca *et al.*, Wolfram syndrome 1 gene negatively regulates ER stress signaling in rodent and human cells. *J. Clin. Invest.* **120**, 744–755 (2010).
12. M. Cagalinec *et al.*, Role of mitochondrial dynamics in neuronal development: Mechanism for Wolfram syndrome. *PLoS Biol.* **14**, e1002511 (2016).
13. D. Takei *et al.*, WFS1 protein modulates the free Ca(2+) concentration in the endoplasmic reticulum. *FEBS Lett.* **580**, 5635–5640 (2006).

14. S. Lu *et al*., A calcium-dependent protease as a potential therapeutic target for Wolfram syndrome. *Proc. Natl. Acad. Sci. U.S.A.* **111**, E5292–E5301 (2014).
15. C. Angebault *et al*., ER-mitochondria cross-talk is regulated by the Ca^{2+} sensor NCS1 and is impaired in Wolfram syndrome. *Sci. Signal.* **11**, eaaq1380 (2018).
16. S. Orrenius, B. Zhivotovsky, P. Nicotera, Regulation of cell death: The calcium-apoptosis link. *Nat. Rev. Mol. Cell Biol.* **4**, 552–565 (2003).
17. C. J. Huang *et al*., Calcium-activated calpain-2 is a mediator of beta cell dysfunction and apoptosis in type 2 diabetes. *J. Biol. Chem.* **285**, 339–348 (2010).
18. S. A. Soleimanpour *et al*., Calcineurin signaling regulates human islet beta-cell survival. *J. Biol. Chem.* **285**, 40050–40059 (2010).
19. B. P. Somesh *et al*., Chronic glucolipotoxic conditions in pancreatic islets impair insulin secretion due to dysregulated calcium dynamics, glucose responsiveness and mitochondrial activity. *BMC Cell Biol.* **14**, 31 (2013).
20. F. M. Qureshi, E. A. Dejene, K. L. Corbin, C. S. Nunemaker, Stress-induced dissociations between intracellular calcium signaling and insulin secretion in pancreatic islets. *Cell Calcium* **57**, 366–375 (2015).
21. P. Gilon, H. Y. Chae, G. A. Rutter, M. A. Ravier, Calcium signaling in pancreatic β-cells in health and in type 2 diabetes. *Cell Calcium* **56**, 340–361 (2014).
22. S. Magi *et al*., Intracellular calcium dysregulation: Implications for Alzheimer's disease. *BioMed Res. Int.* **2016**, 6701324 (2016).
23. G. R. Monteith, N. Prevarskaya, S. J. Roberts-Thomson, The calcium-cancer signalling nexus. *Nat. Rev. Cancer* **17**, 367–380 (2017).
24. S. G. Massry, M. Smogorzewski, Role of elevated cytosolic calcium in the pathogenesis of complications in diabetes mellitus. *Miner. Electrolyte Metab.* **23**, 253–260 (1997).
25. A. P. Arruda, G. S. Hotamisligil, Calcium homeostasis and organelle function in the pathogenesis of obesity and diabetes. *Cell Metab.* **22**, 381–397 (2015).
26. A. Raturi, T. Simmen, Where the endoplasmic reticulum and the mitochondrion tie the knot: The mitochondria-associated membrane (MAM). *Biochim. Biophys. Acta* **1833**, 213–224 (2013).
27. E. Area-Gomez *et al*., A key role for MAM in mediating mitochondrial dysfunction in Alzheimer disease. *Cell Death Dis.* **9**, 335 (2018).
28. E. Tubbs *et al*., Mitochondria-associated endoplasmic reticulum membrane (MAM) integrity is required for insulin signaling and is implicated in hepatic insulin resistance. *Diabetes* **63**, 3279–3294 (2014).
29. C. Thivolet, G. Vial, R. Cassel, J. Rieusset, A. M. Madec, Reduction of endoplasmic reticulum–mitochondria interactions in beta cells from patients with type 2 diabetes. *PLoS One* **12**, e0182027 (2017).
30. A. Zhang *et al*., Quantitative proteomic analyses of human cytomegalovirus-induced restructuring of endoplasmic reticulum-mitochondrial contacts at late times of infection. *Mol. Cell. Proteomics* **10**, M111.009936 (2011).
31. C. N. Poston, S. C. Krishnan, C. R. Bazemore-Walker, In-depth proteomic analysis of mammalian mitochondria-associated membranes (MAM). *J. Proteomics* **79**, 219–230 (2013).
32. S. M. Horner, C. Wilkins, S. Badil, J. Iskarpatyoti, M. Gale Jr., Proteomic analysis of mitochondrial-associated ER membranes (MAM) during RNA virus infection reveals dynamic changes in protein and organelle trafficking. *PLoS One* **10**, e0117963 (2015).
33. M. Z. Khaldi, Y. Guiot, P. Gilon, J. C. Henquin, J. C. Jonas, Increased glucose sensitivity of both triggering and amplifying pathways of insulin secretion in rat islets cultured for 1 wk in high glucose. *Am. J. Physiol. Endocrinol. Metab.* **287**, E207–E217 (2004).
34. T. Tsuboi, M. A. Ravier, L. E. Parton, G. A. Rutter, Sustained exposure to high glucose concentrations modifies glucose signaling and the mechanics of secretory vesicle fusion in primary rat pancreatic beta-cells. *Diabetes* **55**, 1057–1065 (2006).
35. C. Tang *et al*., Glucose-induced beta cell dysfunction in vivo in rats: Link between oxidative stress and endoplasmic reticulum stress. *Diabetologia* **55**, 1366–1379 (2012).
36. T. Y. Nakamura, S. Nakao, S. Wakabayashi, Emerging roles of neuronal Ca^{2+} sensor-1 in cardiac and neuronal tissues: A mini review. *Front. Mol. Neurosci.* **12**, 56 (2019).
37. T. Y. Nakamura *et al*., Novel role of neuronal $Ca2^{+}$ sensor-1 as a survival factor up-regulated in injured neurons. *J. Cell Biol.* **172**, 1081–1091 (2006).
38. J. Gromada *et al*., Neuronal calcium sensor-1 potentiates glucose-dependent exocytosis in pancreatic beta cells through activation of phosphatidylinositol 4-kinase beta. *Proc. Natl. Acad. Sci. U.S.A.* **102**, 10303–10308 (2005).
39. T. Y. Nakamura, S. Nakao, S. Wakabayashi, Neuronal Ca^{2+} sensor-1 contributes to stress tolerance in cardiomyocytes via activation of mitochondrial detoxification pathways. *J. Mol. Cell. Cardiol.* **99**, 23–34 (2016).
40. J. H. Benbow *et al*., Inhibition of paclitaxel-induced decreases in calcium signaling. *J. Biol. Chem.* **287**, 37907–37916 (2012).
41. A. Mansilla *et al*., Interference of the complex between NCS-1 and Ric8a with phenothiazines regulates synaptic function and is an approach for fragile X syndrome. *Proc. Natl. Acad. Sci. U.S.A.* **114**, E999–E1008 (2017).
42. A. Karasik *et al*., Genetically programmed selective islet beta-cell loss in diabetic subjects with Wolfram's syndrome. *Diabetes Care* **12**, 135–138 (1989).
43. A. C. Riggs *et al*., Mice conditionally lacking the Wolfram gene in pancreatic islet beta cells exhibit diabetes as a result of enhanced endoplasmic reticulum stress and apoptosis. *Diabetologia* **48**, 2313–2321 (2005).
44. Y. Ono, T. C. Saido, H. Sorimachi, Calpain research for drug discovery: Challenges and potential. *Nat. Rev. Drug Discov.* **15**, 854–876 (2016).
45. T. James, D. Matzelle, R. Bartus, E. L. Hogan, N. L. Banik, New inhibitors of calpain prevent degradation of cytoskeletal and myelin proteins in spinal cord in vitro. *J. Neurosci. Res.* **51**, 218–222 (1998).
46. C. A. Huser, M. E. Davies, Calcium signaling leads to mitochondrial depolarization in impact-induced chondrocyte death in equine articular cartilage explants. *Arthritis Rheum.* **56**, 2322–2334 (2007).
47. K. Motani *et al*., Activation of ASC induces apoptosis or necrosis, depending on the cell type, and causes tumor eradication. *Cancer Sci.* **101**, 1822–1827 (2010).
48. F. Paquet-Durand *et al*., Photoreceptor rescue and toxicity induced by different calpain inhibitors. *J. Neurochem.* **115**, 930–940 (2010).
49. R. T. Bartus *et al*., Calpain inhibitor AK295 protects neurons from focal brain ischemia. Effects of postocclusion intra-arterial administration. *Stroke* **25**, 2265–2270 (1994).
50. R. L. DeBiasi, C. L. Edelstein, B. Sherry, K. L. Tyler, Calpain inhibition protects against virus-induced apoptotic myocardial injury. *J. Virol.* **75**, 351–361 (2001).
51. P. Rolan, M. Hutchinson, K. Johnson, Ibudilast: A review of its pharmacology, efficacy and safety in respiratory and neurological disease. *Expert Opin. Pharmacother.* **10**, 2897–2904 (2009).
52. H. Ishihara *et al*., Disruption of the WFS1 gene in mice causes progressive beta-cell loss and impaired stimulus-secretion coupling in insulin secretion. *Hum. Mol. Genet.* **13**, 1159–1170 (2004).
53. M. Plaas *et al*., Wfs1-deficient rats develop primary symptoms of Wolfram syndrome: Insulin-dependent diabetes, optic nerve atrophy and medullary degeneration. *Sci. Rep.* **7**, 10220 (2017).
54. D. Waddleton *et al*., Phosphodiesterase 3 and 4 comprise the major cAMP metabolizing enzymes responsible for insulin secretion in INS-1 (832/13) cells and rat islets. *Biochem. Pharmacol.* **76**, 884–893 (2008).
55. R. N. Kulkarni *et al*., Tissue-specific knockout of the insulin receptor in pancreatic beta cells creates an insulin secretory defect similar to that in type 2 diabetes. *Cell* **96**, 329–339 (1999).
56. S. Xuan *et al*., Defective insulin secretion in pancreatic beta cells lacking type 1 IGF receptor. *J. Clin. Invest.* **110**, 1011–1019 (2002).
57. I. B. Leibiger, B. Leibiger, P. O. Berggren, Insulin signaling in the pancreatic beta-cell. *Annu. Rev. Nutr.* **28**, 233–251 (2008).
58. C. Schlecker *et al*., Neuronal calcium sensor-1 enhancement of InsP3 receptor activity is inhibited by therapeutic levels of lithium. *J. Clin. Invest.* **116**, 1668–1674 (2006).
59. L. D. Nguyen, E. T. Petri, L. K. Huynh, B. E. Ehrlich, Characterization of NCS1-InsP3R1 interaction and its functional significance. *J. Biol. Chem.* **294**, 18923–18933 (2019).
60. A. A. Osman *et al*., Wolframin expression induces novel ion channel activity in endoplasmic reticulum membranes and increases intracellular calcium. *J. Biol. Chem.* **278**, 52755–52762 (2003).
61. T. Yuan, B. Lupse, K. Maedler, A. Ardestani, mTORC2 signaling: A path for pancreatic β cell's growth and function. *J. Mol. Biol.* **430**, 904–918 (2018).
62. E. Bernal-Mizrachi *et al*., Defective insulin secretion and increased susceptibility to experimental diabetes are induced by reduced Akt activity in pancreatic islet beta cells. *J. Clin. Invest.* **114**, 928–936 (2004).
63. B. A. Hemmings, D. F. Restuccia, PI3K-PKB/Akt pathway. *Cold Spring Harb. Perspect. Biol.* **4**, a011189 (2012).
64. R. L. Tuttle *et al*., Regulation of pancreatic beta-cell growth and survival by the serine/threonine protein kinase Akt1/PKBalpha. *Nat. Med.* **7**, 1133–1137 (2001).
65. N. M. Conus, B. A. Hemmings, R. B. Pearson, Differential regulation by calcium reveals distinct signaling requirements for the activation of Akt and p70S6k. *J. Biol. Chem.* **273**, 4776–4782 (1998).
66. J. K. Kang *et al*., Increased intracellular Ca^{2+} concentrations prevent membrane localization of PH domains through the formation of Ca^{2+}-phosphoinositides. *Proc. Natl. Acad. Sci. U.S.A.* **114**, 11926–11931 (2017).
67. A. Kowluru, A. Matti, Hyperactivation of protein phosphatase 2A in models of glucolipotoxicity and diabetes: Potential mechanisms and functional consequences. *Biochem. Pharmacol.* **84**, 591–597 (2012).
68. P. P. Ruvolo, The broken "off" switch in cancer signaling: PP2A as a regulator of tumorigenesis, drug resistance, and immune surveillance. *BBA Clin.* **6**, 87–99 (2016).
69. X. Huang, G. Liu, J. Guo, Z. Su, The PI3K/AKT pathway in obesity and type 2 diabetes. *Int. J. Biol. Sci.* **14**, 1483–1496 (2018).
70. O. Ratai, J. Hermainski, K. Ravichandran, O. Pongs, NCS-1 deficiency is associated with obesity and diabetes type 2 in mice. *Front. Mol. Neurosci.* **12**, 78 (2019).
71. D. E. Goll, V. F. Thompson, H. Li, W. Wei, J. Cong, The calpain system. *Physiol. Rev.* **83**, 731–801 (2003).
72. Z. Li *et al*., Novel peptidyl alpha-keto amide inhibitors of calpains and other cysteine proteases. *J. Med. Chem.* **39**, 4089–4098 (1996).
73. T. Yamashima, Can the "calpain-cathepsin hypothesis" explain Alzheimer neuronal death? *Ageing Res. Rev.* **32**, 169–179 (2016).
74. Y. Li, Y. Li, Q. Feng, M. Arnold, T. Peng, Calpain activation contributes to hyperglycaemia-induced apoptosis in cardiomyocytes. *Cardiovasc. Res.* **84**, 100–110 (2009).
75. T. Gurlo *et al*., β cell-specific increased expression of calpastatin prevents diabetes induced by islet amyloid polypeptide toxicity. *JCI Insight* **1**, e89590 (2016).
76. U. S. Jhala *et al*., cAMP promotes pancreatic beta-cell survival via CREB-mediated induction of IRS2. *Genes Dev.* **17**, 1575–1580 (2003).
77. L. R. Landa Jr. *et al*., Interplay of Ca^{2+} and cAMP signaling in the insulin-secreting MIN6 beta-cell line. *J. Biol. Chem.* **280**, 31294–31302 (2005).
78. K. Yan, L. N. Gao, Y. L. Cui, Y. Zhang, X. Zhou, The cyclic AMP signaling pathway: Exploring targets for successful drug discovery (review). *Mol. Med. Rep.* **13**, 3715–3723 (2016).
79. A. Ledeboer *et al*., The glial modulatory drug AV411 attenuates mechanical allodynia in rat models of neuropathic pain. *Neuron Glia Biol.* **2**, 279–291 (2006).

80. A. T. Hama, A. Broadhead, D. S. Lorrain, J. Sagen, The antinociceptive effect of the asthma drug ibudilast in rat models of peripheral and central neuropathic pain. *J. Neurotrauma* **29**, 600–610 (2012).
81. M. Mo, I. Erdelyi, K. Szigeti-Buck, J. H. Benbow, B. E. Ehrlich, Prevention of paclitaxel-induced peripheral neuropathy by lithium pretreatment. *FASEB J.* **26**, 4696–4709 (2012).
82. R. J. Fox *et al*.; NN102/SPRINT-MS Trial Investigators, Phase 2 trial of ibudilast in progressive multiple sclerosis. *N. Engl. J. Med.* **379**, 846–855 (2018).
83. US National Library of Medicine, Evaluation of MN-166 (ibudilast) for 12 months followed by an open-label extension for 6 months in patients with ALS. https://clinicaltrials.gov/ct2/show/NCT04057898. Accessed June 8, 2020.
84. J. Levy, J. R. Gavin 3rd, J. R. Sowers, Diabetes mellitus: A disease of abnormal cellular calcium metabolism? *Am. J. Med.* **96**, 260–273 (1994).
85. M. P. Mattson, Calcium and neurodegeneration. *Aging Cell* **6**, 337–350 (2007).
86. E. Pchitskaya, E. Popugaeva, I. Bezprozvanny, Calcium signaling and molecular mechanisms underlying neurodegenerative diseases. *Cell Calcium* **70**, 87–94 (2018).
87. I. Pomytkin *et al*., Insulin receptor in the brain: Mechanisms of activation and the role in the CNS pathology and treatment. *CNS Neurosci. Ther.* **24**, 763–774 (2018).
88. S. R. Jesinkey *et al*., Mitochondrial GTP links nutrient sensing to beta cell health, mitochondrial morphology, and insulin secretion independent of OxPhos. *Cell Rep.* **28**, 759–772.e10 (2019).